Supplementary Information

Dual Channel chromo/ fluorogenic chemosensors for cyanide and fluoride ions- an example of in situ acid catalysis of strecker reaction for cyanide ion chemodosimetry.

Sanyog Sharma, Maninder Singh Hundal* and Geeta Hundal*

Department of Chemistry, Guru Nanak Dev University, Amritsar-143005,

Punjab, India

Email Address: geetahundal@yahoo.com; hundal_chem@yahoo.com

Table of Contents

Synthetic Procedures and Characterization.

Scheme S1. Synthesis of sensor **(4)** and **(5): Schiff Base Condensation Reaction.**

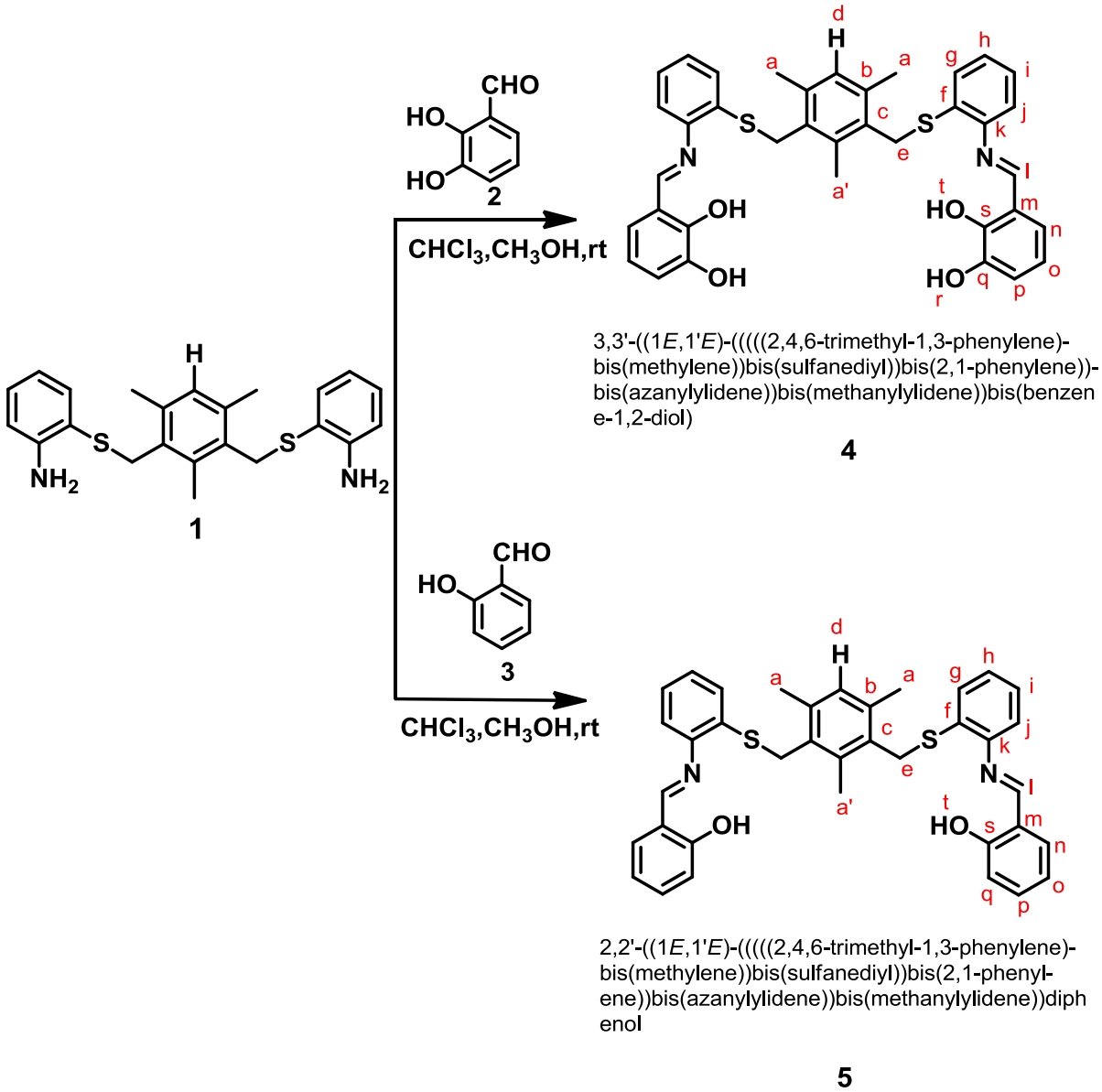

3,3'-((1*E*,1'*E*)-(((((2,4,6-trimethyl-1,3-phenylene)-bis(methylene))bis(sulfanediyl))bis(2,1-phenylene))-bis(azanylylidene))bis(methanylylidene))bis(benzene-1,2-diol)

4

2,2'-((1*E*,1'*E*)-(((((2,4,6-trimethyl-1,3-phenylene)-bis(methylene))bis(sulfanediyl))bis(2,1-phenylene))bis(azanylylidene))bis(methanylylidene))diphenol

5

Scheme S2. Synthesis of chemodosimeters **(6)** and **(7): Strecker Reaction.**

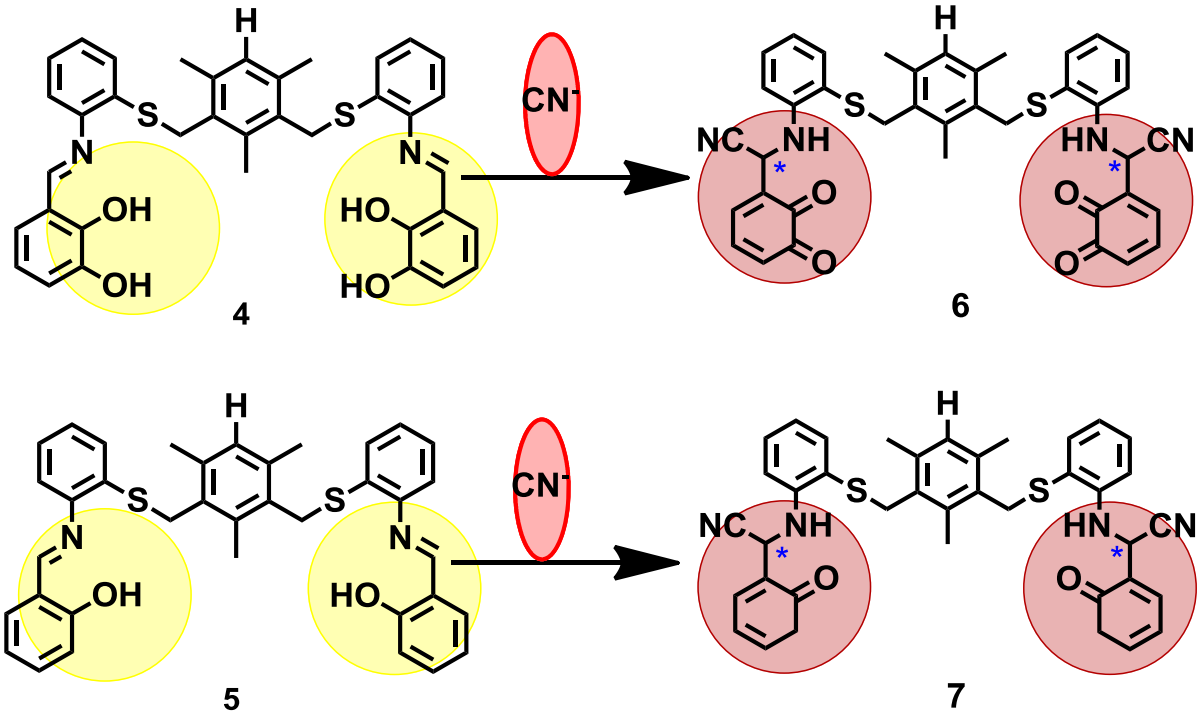

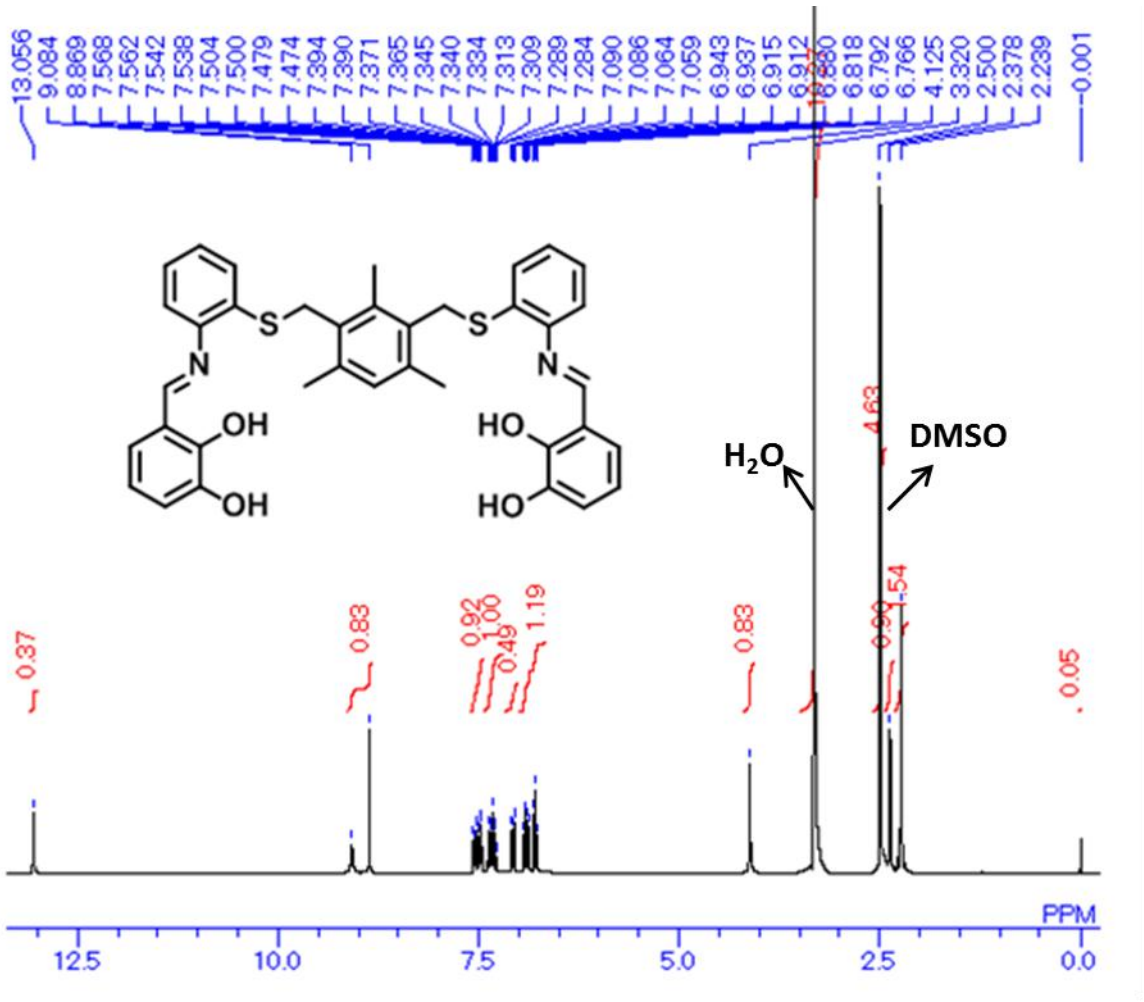

Fig. S1. ^{1}H NMR spectrum of compound (4).

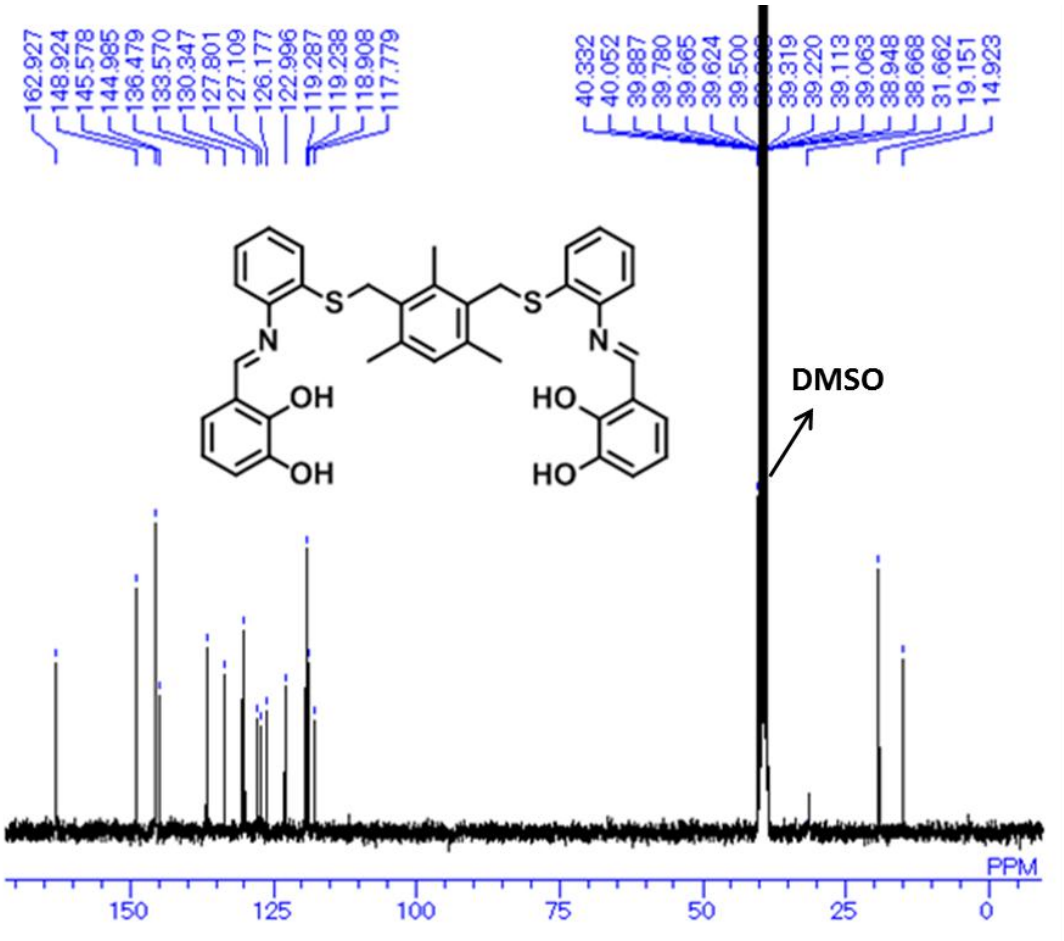

Fig. S2. ^{13}C NMR spectrum of compound (4).

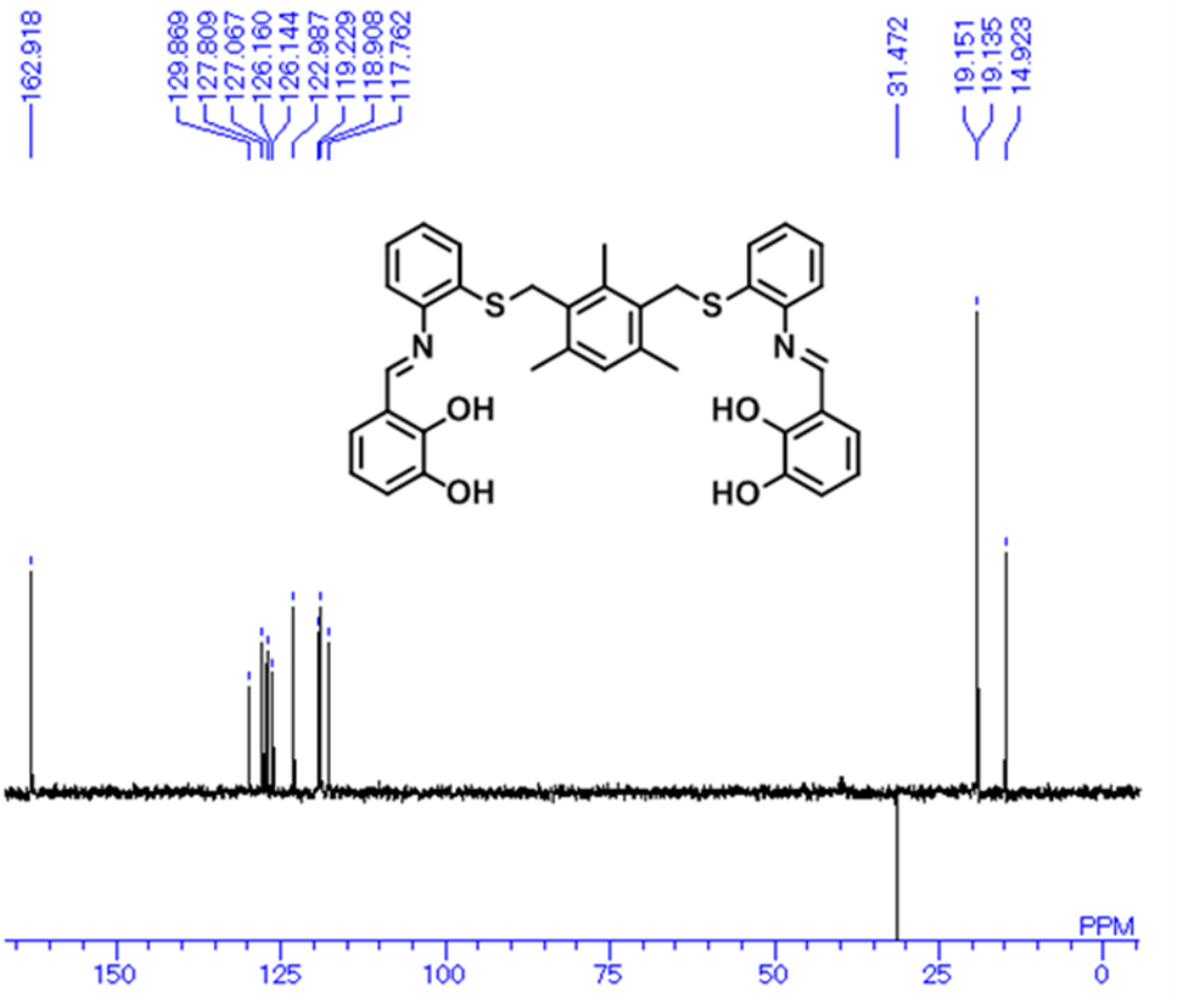

Fig. S3. DEPT-135 spectrum of compound (4).

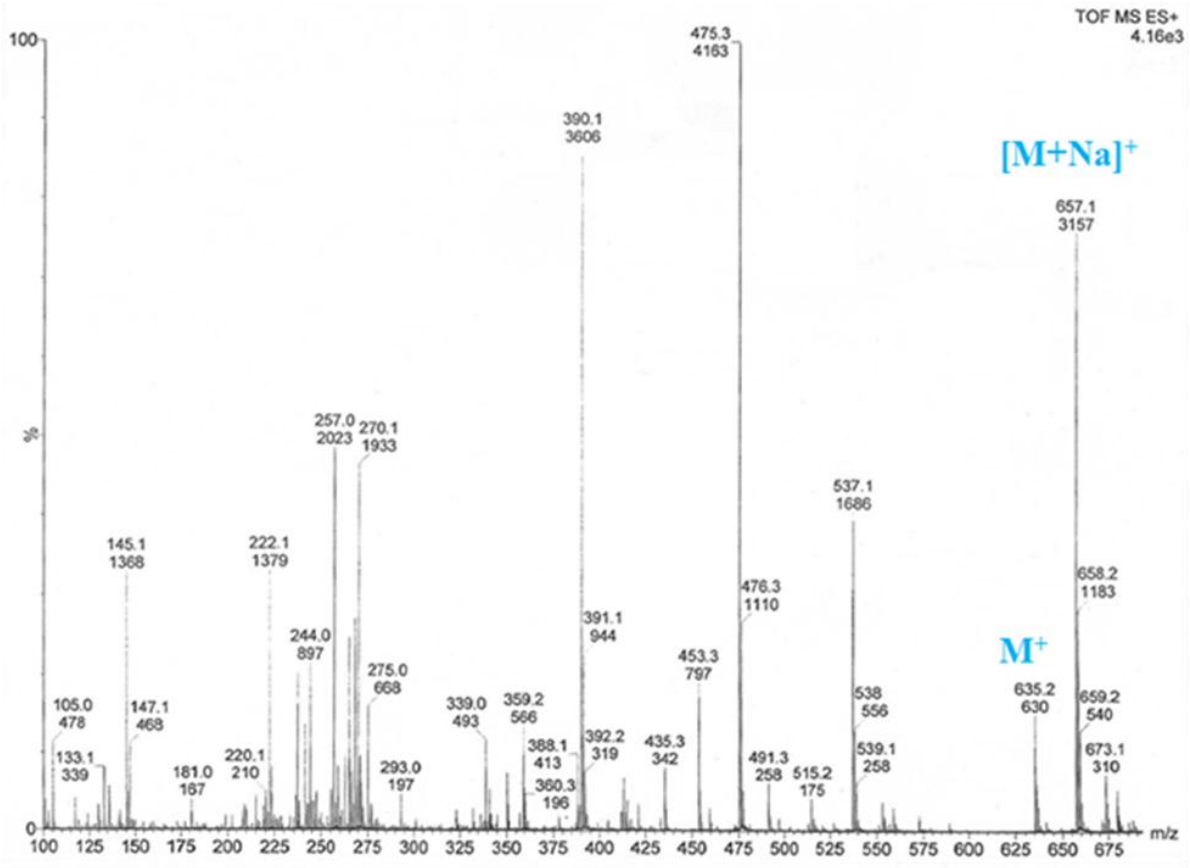

Fig. S4. Mass Spectrum of compound (4).

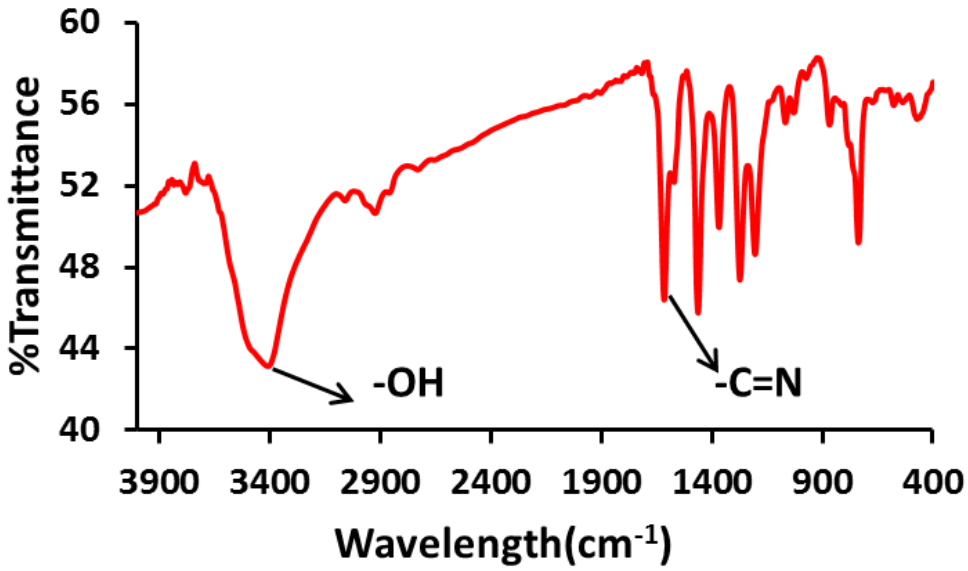

Fig. S5. IR Spectrum of compound (4).

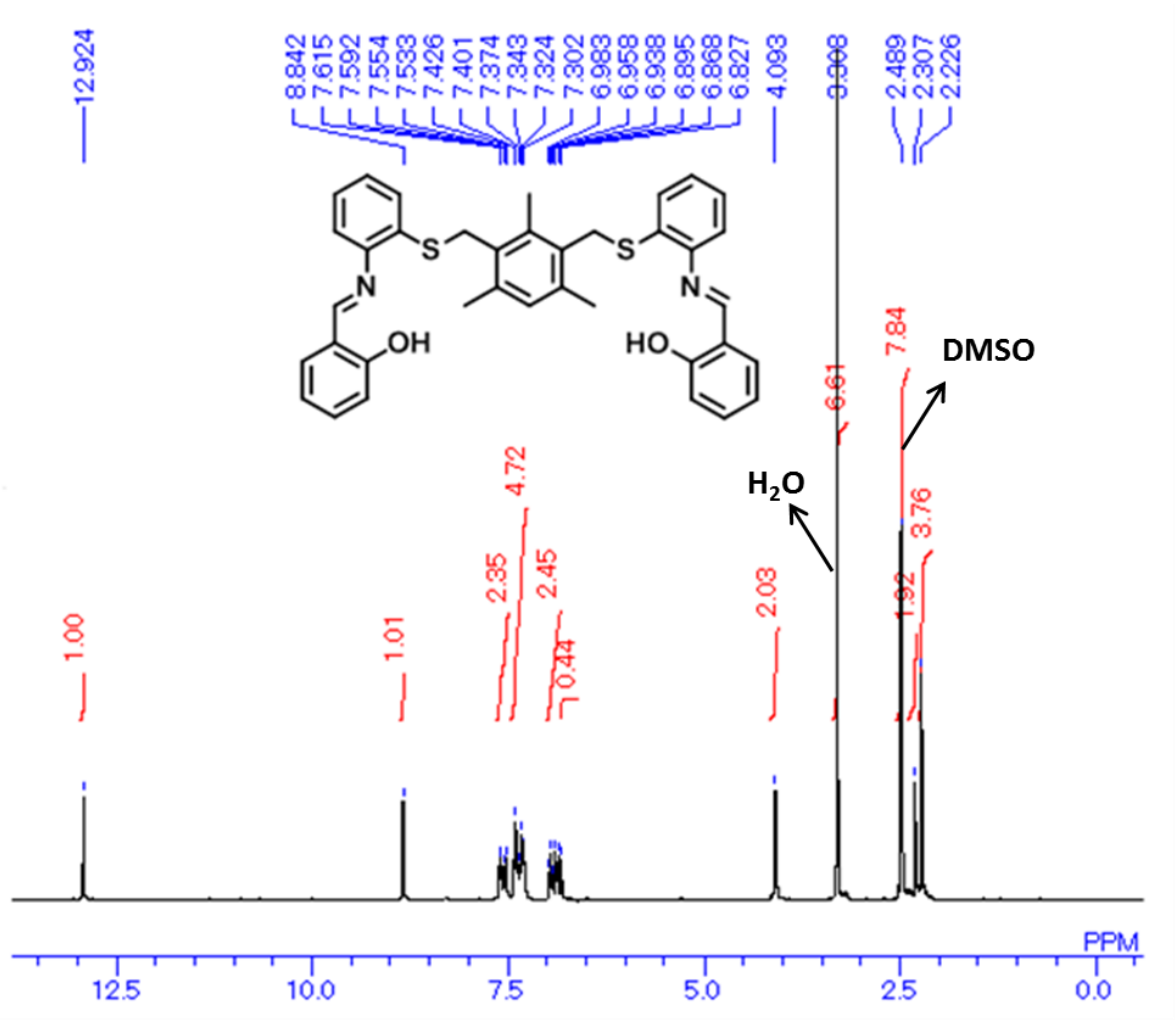

Fig. S6. ^{1}H NMR spectrum of compound (5).

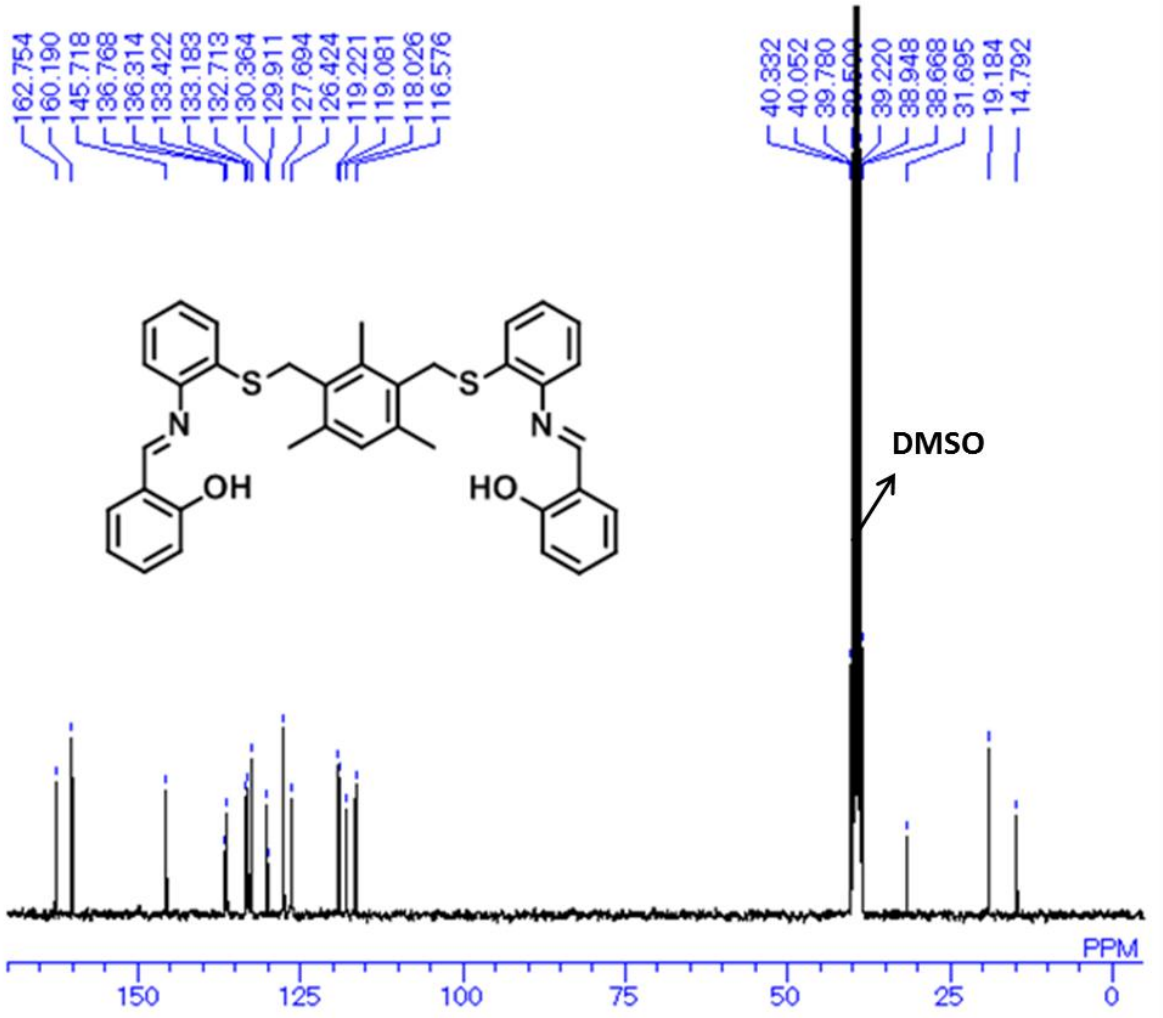

Fig. S7. ^{13}C NMR spectrum of compound (5).

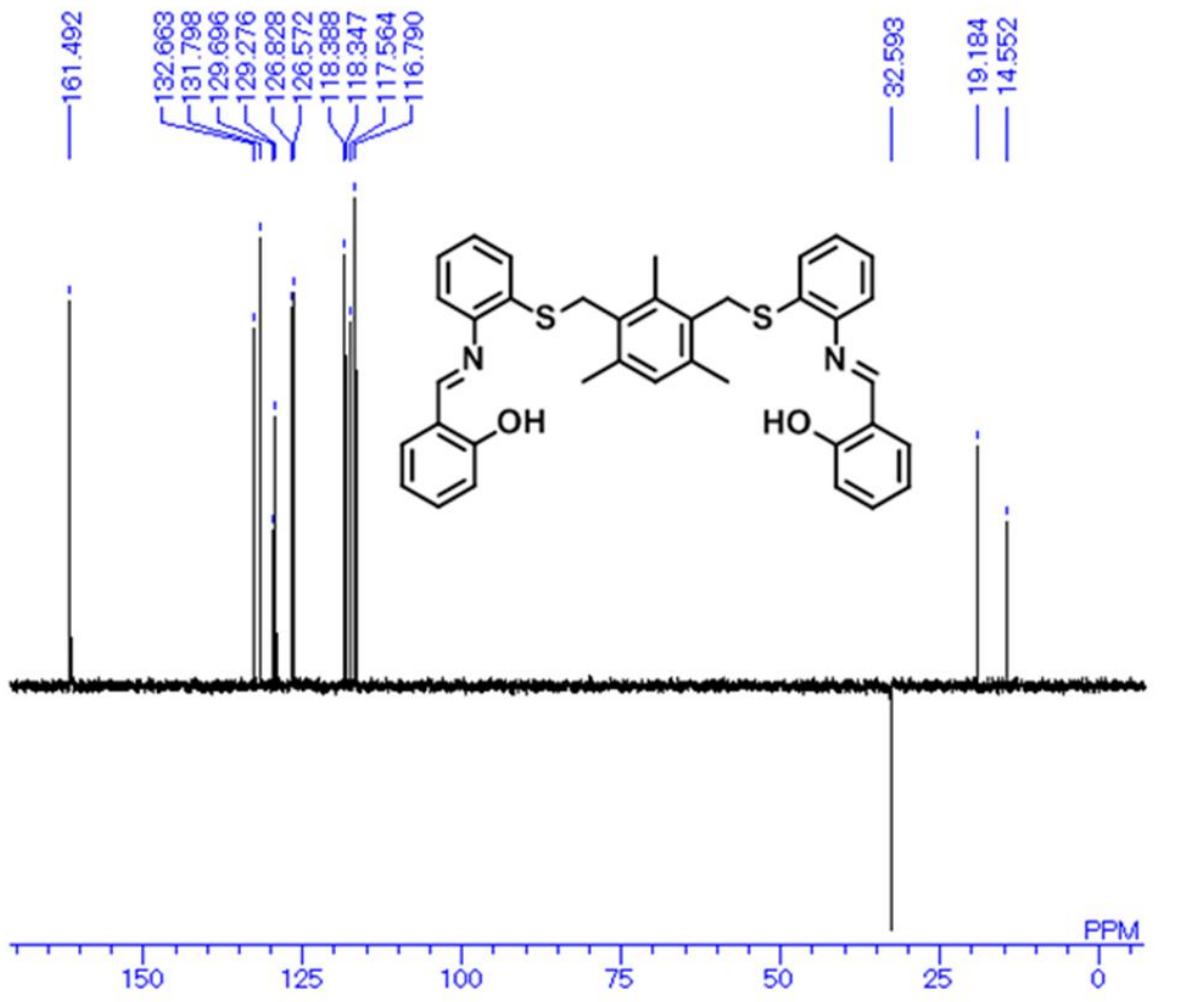

Fig. S8. DEPT-135 spectrum of compound (5).

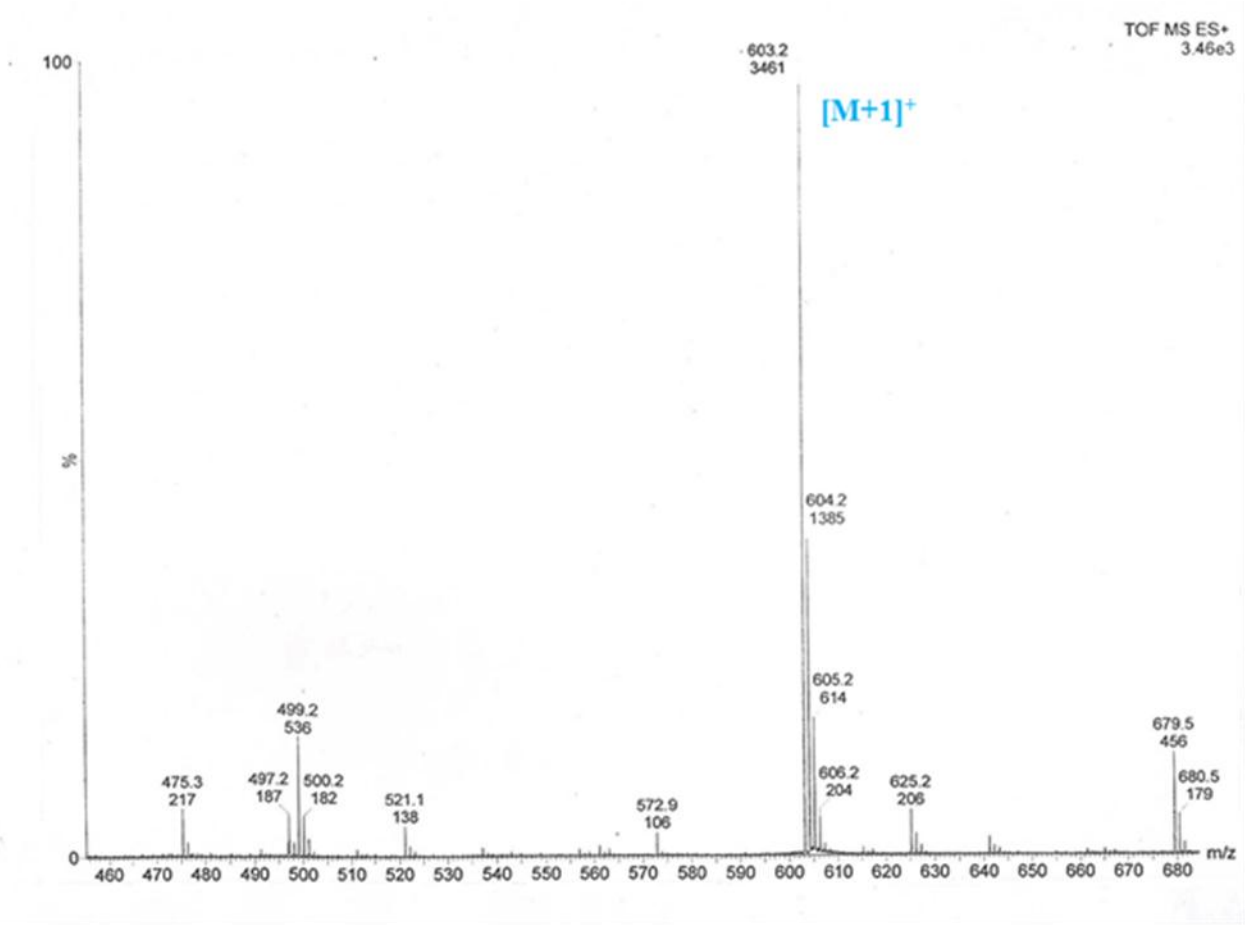

Fig. S9. Mass Spectrum of compound (5).

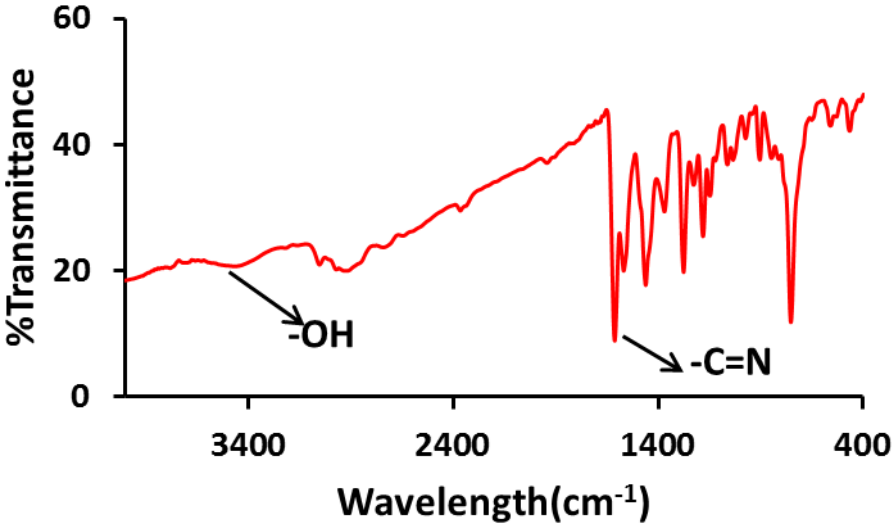

Fig. S10. IR Spectrum of compound (5).

Molecular and crystal structure of (5). The molecular structure of (**5**) (Fig. 1) shows that the dipodal molecule has an approximate 'U' shaped conformation with the central anchor phenyl ring forming the base. The torsion angle about C-S bonds are C7-S1 176.35 and C21-S2 159.48° with the dihedral angles between the central ring and the 2-amino-thiophenol ring being 77.2(1) and 51.8(2)°, respectively. The phenyl rings of 2-aminothiophenol and salicylaldehyde moieties on both the arms are rotated by 2.3(2) and 21.3(2)°, respectively with respect to each other. Two planes passing through the two phenyl rings and the imine group on both the arms showed an interplanar angle of 85.7(1) between them and are making dihedral angles 75.9(1) and 60.6(1)° with the central phenyl ring. All these values show that the two arms of the dipodand in the 'U' conformation are not parallel but twisted with respect to each other and one of the arms (with C21-S2 bond) is rather *gauche* than being perpendicular to the central ring (Fig. S11) unlike the other arm. This distortion is probably there to make room for the CCl_4 solvent molecule which lies close to the latter making C-H…Cl H-bonding interactions and due to the packing requirements (Fig. S11). There are strong intramolecular H-bonding interactions between the OH groups and imine nitrogens as well as the S atoms which are supporting this conformation.

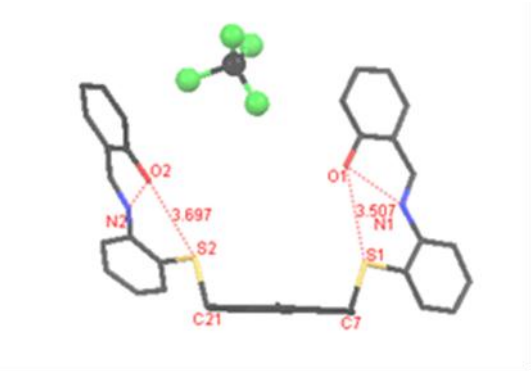

Fig. S11. Showing the 'U' conformation of the molecule and intramolecular H-bonding interactions in (5).

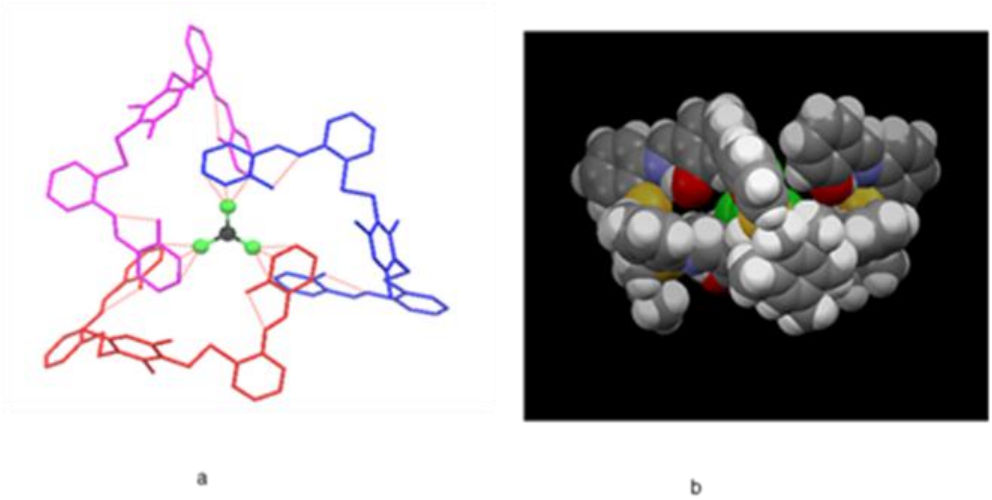

Fig. S12. Showing the intramolecular H-bonding interactions holding the solvent CCl_4 molecule (black and green balls) in the pseudo-cavity of the trimeric unit (a) stick and ball-n-stick (b) space-filled representations.

The molecules are arranged in the form of H-bonded trimers around the disordered CCl_4 solvent molecule whose one C-Cl bond (C38-Cl1) coincides with the three fold axis along the *c* axis (Fig. S12a). Each Cl2 lying in the trigonal plane is H-bonded to C31 and C32 (C31…Cl2^a 3.247, C32…Cl2 ^{a} 3.402, a = x, -1+y,z) whereas each Cl2' is H-bonded to C24 phenylene carbon. Thus the solvent molecule is securely held in the hydrophobic pseudo-cavity of this trimer (Fig. S12b). Each unit cell contains 6 of such trimeric units which are further held to each other by C-H…O kind of weak H-bonding interactions as shown in Fig. S13.

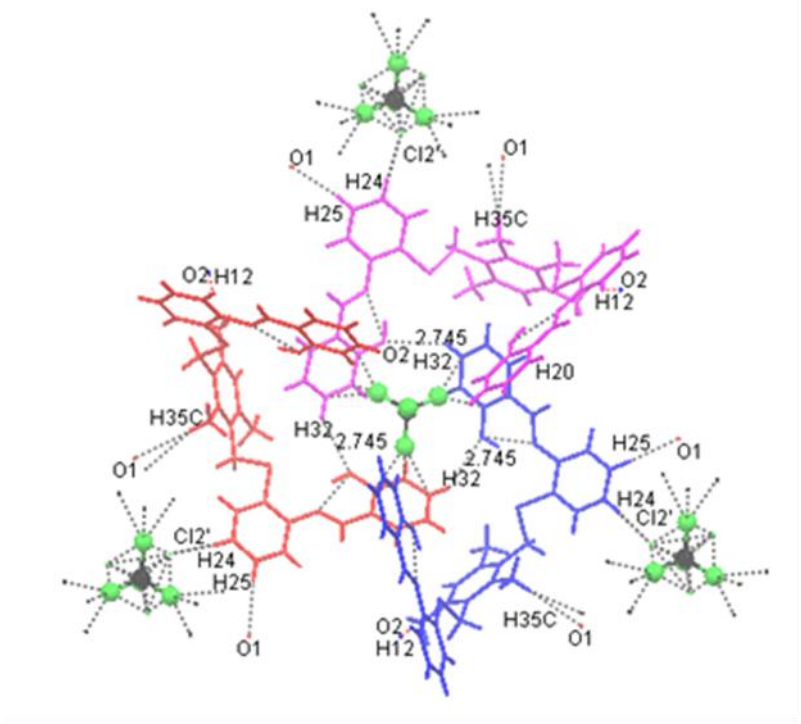

Fig. S13. Showing inter-molecular H-bonding interactions forming the crystal structure.

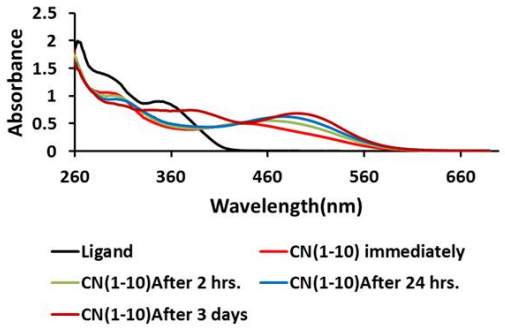

Changes in absorption of (4) with TBACN with time.

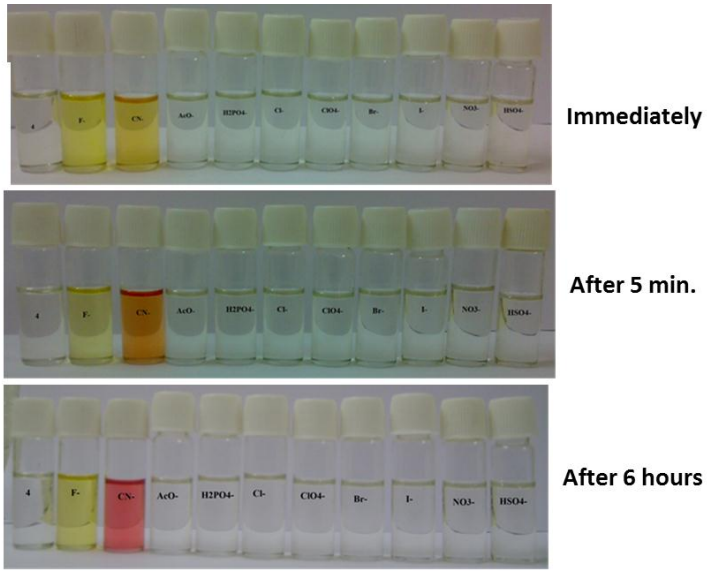

Color changes of (4) with different anions with time

Fig. S14. Showing changes in absorption and colors of (4) on addition of TBA anions with time.

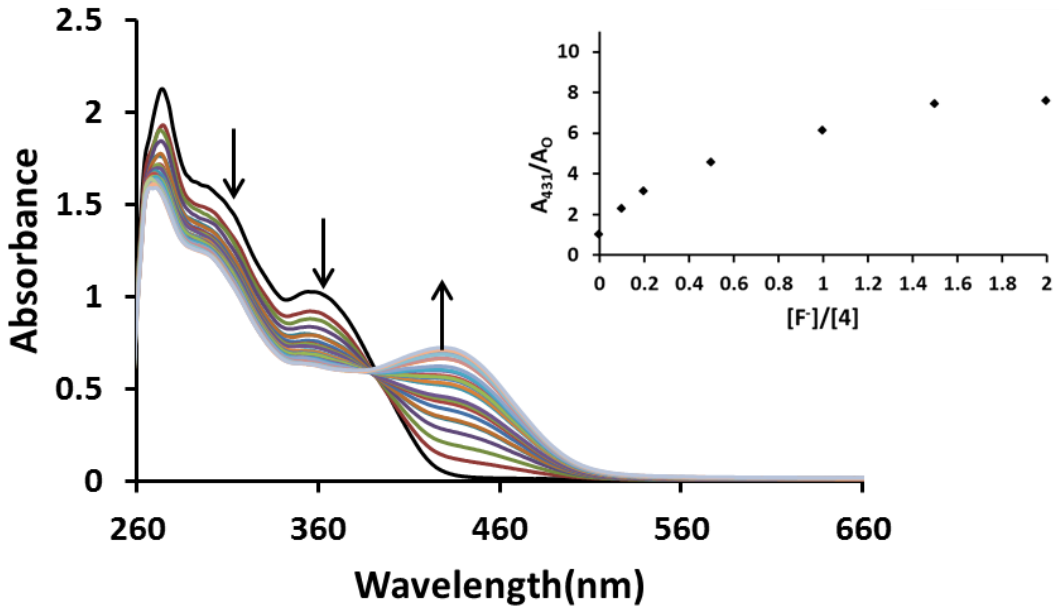

Fig. S15. Changes in UV-vis spectra of sensor 4 (10 µM) upon gradual addition of TBAF (0-100µM). Inset shows chromogenic determination of fluoride detection after stepwise addition of TBAF in DMSO which was found to be less than 1.5µM as significant change appears at 1µM.

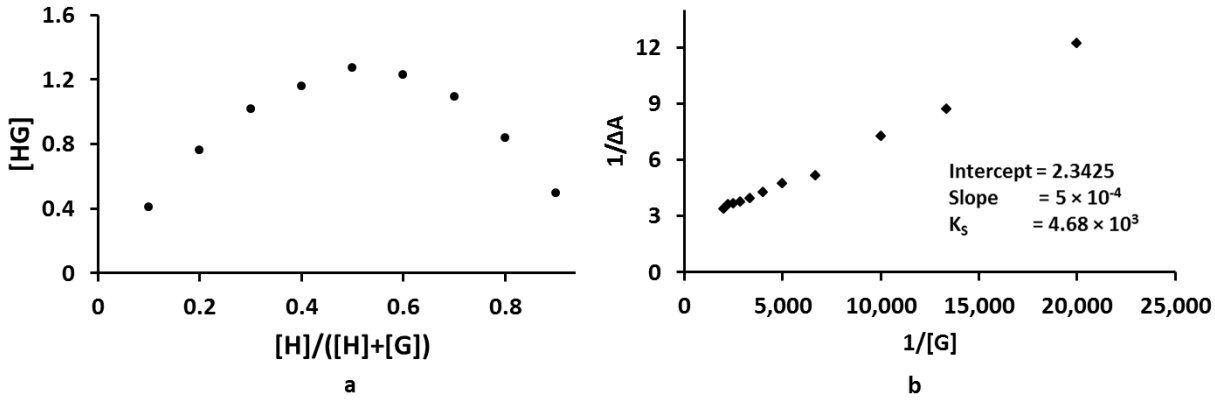

Fig. S16. Stoichiometry and Benesi-Hildebrand plot for (4) with TBAF.

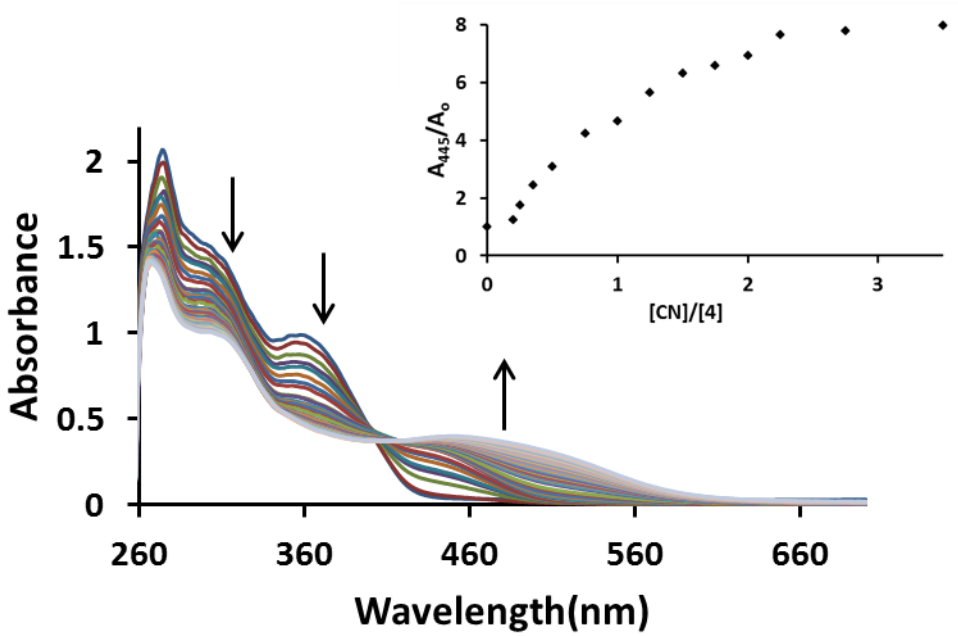

Fig. S17. Changes in UV-vis spectra of sensor 4 (10 µM) upon gradual addition of TBACN (0-100µM) in DMSO. Inset shows chromogenic determination of cyanide detection after stepwise addition of TBACN which was found to be less than 3µM as significant change appears at 2.1µM.

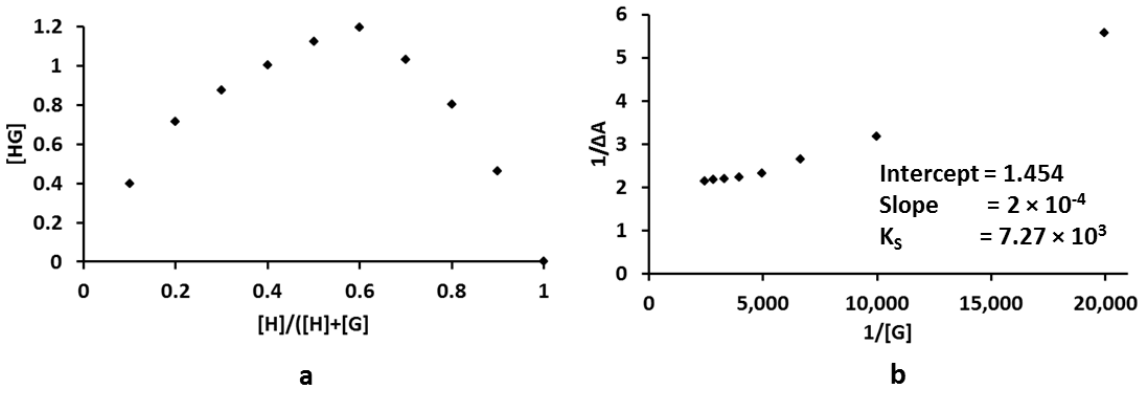

Fig. S18. Stoichiometry and Benesi-Hildebrand plot for (4) with TBACN.

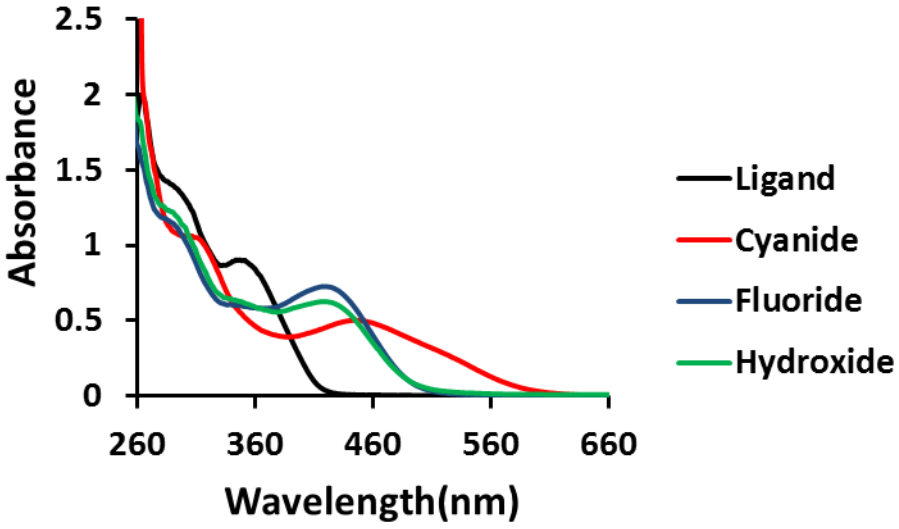

Fig. S19. Changes in UV-vis spectra of (4) (10 μM) with TBAF, TBACN and TBAOH (10 equivalents) in DMSO.

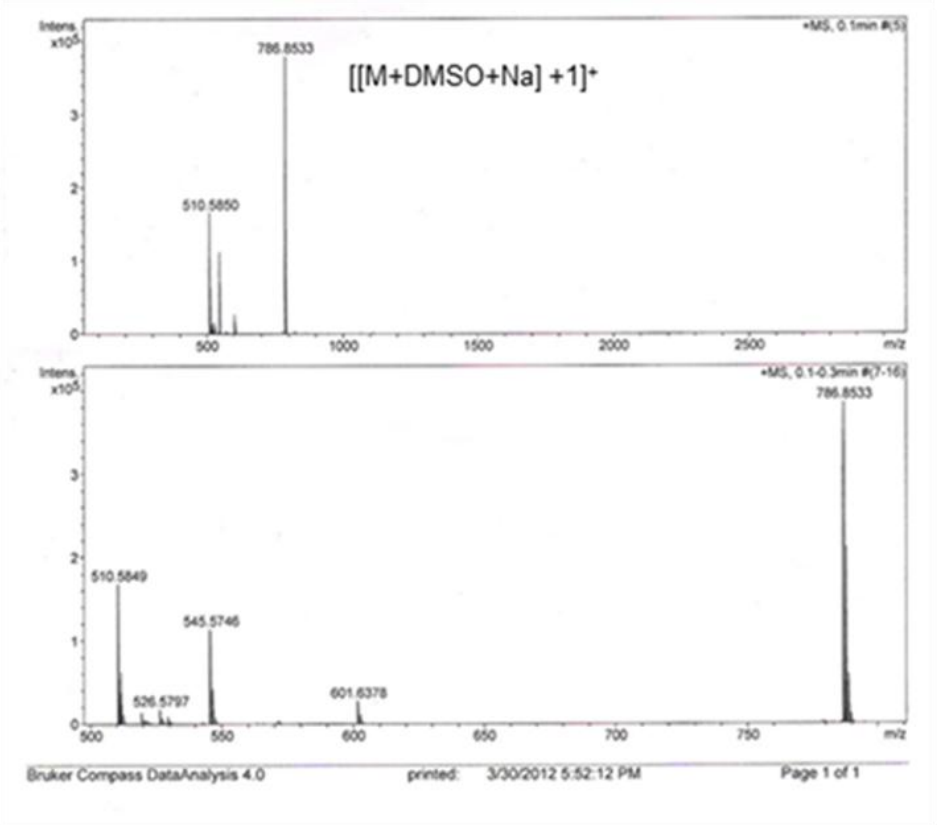

Fig. S20. Mass Spectrum of CN adduct (6) obtained on addition of TBACN in (4) in DMSO.

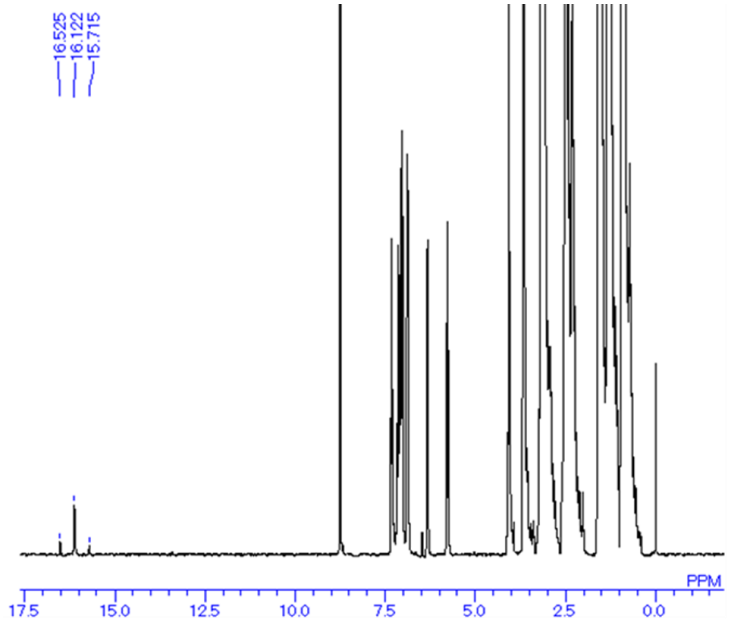

Fig. S21. Showing the triplet characteristic for the presence of $[HF_2]^-$ anion on addition of 10 equiv. of TBAF in 5mM of sensor(4).

(a) Fluorescence color changes for (4) with different anions, Sensor : analyte ratio 1: 10, sensor concn. 5µM

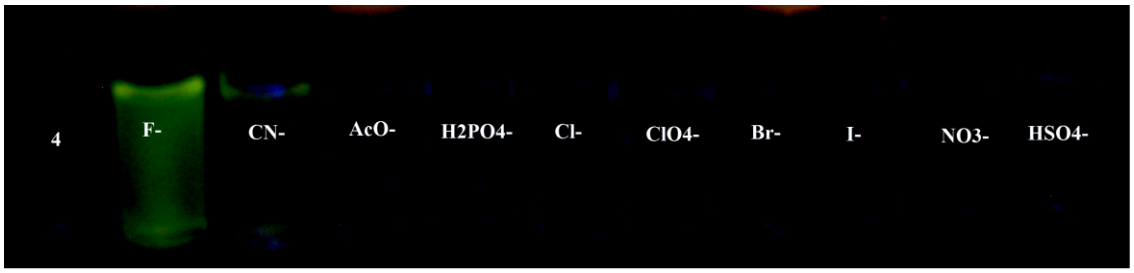

(b) Fluorescence color changes for (5) with different anions, Sensor : analyte ratio 1: 10, sensor concn. 10µM

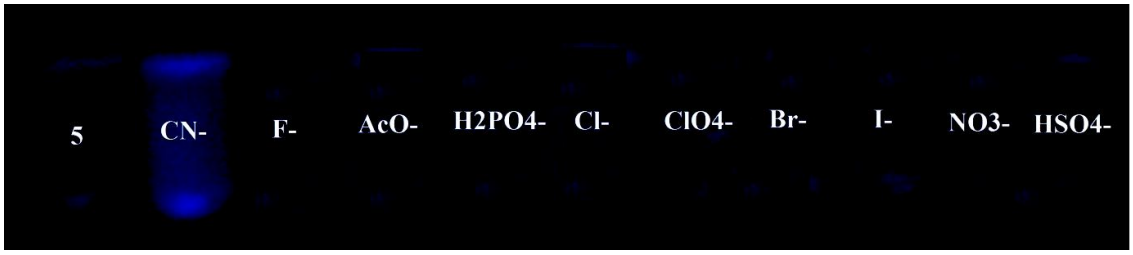

Fig. S22. Fluorescence color changes in (4) above and (5) below, with various anions.

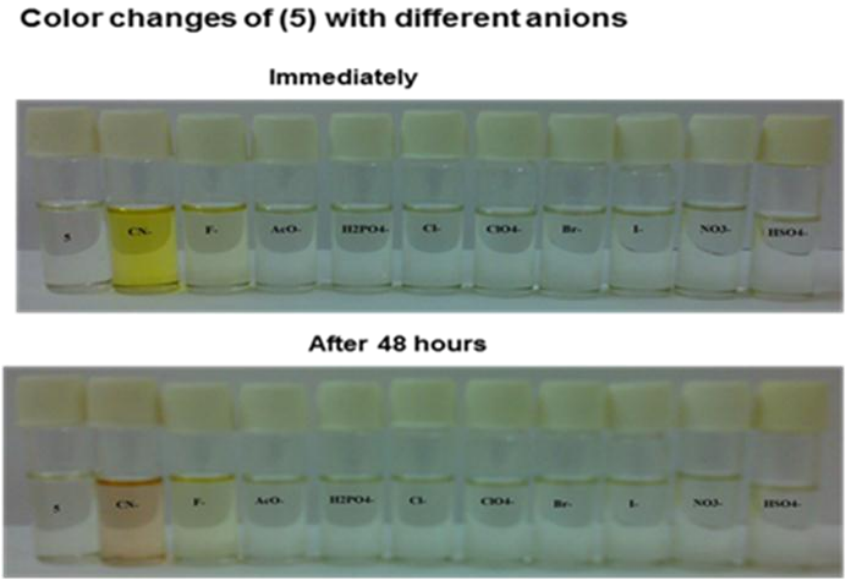

Fig. S23. Visual color changes in (5) in DMSO with various anions.

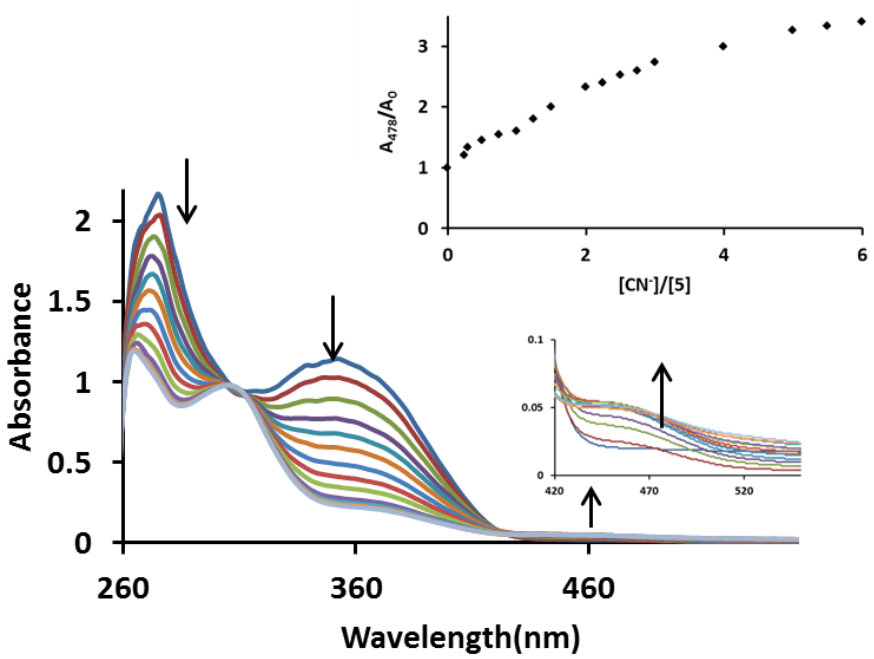

Fig. S24. Showing changes in UV-vis of (5) (10 μM) in DMSO with gradual addition of TBACN, inset- expanded increase in absorbance near 465 nm and chromogenic determination of cyanide detection which was found less than 3μM as significant change appears at 2.5μM.

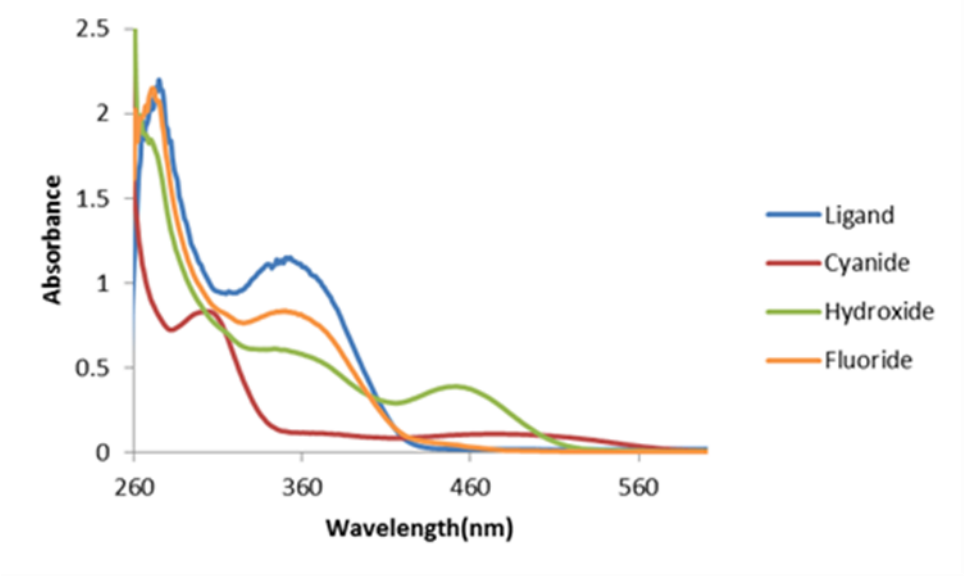

Fig. S25. Showing changes in UV spectrum of (5) with TBA salts of F^-, CN^- and OH^- in DMSO.

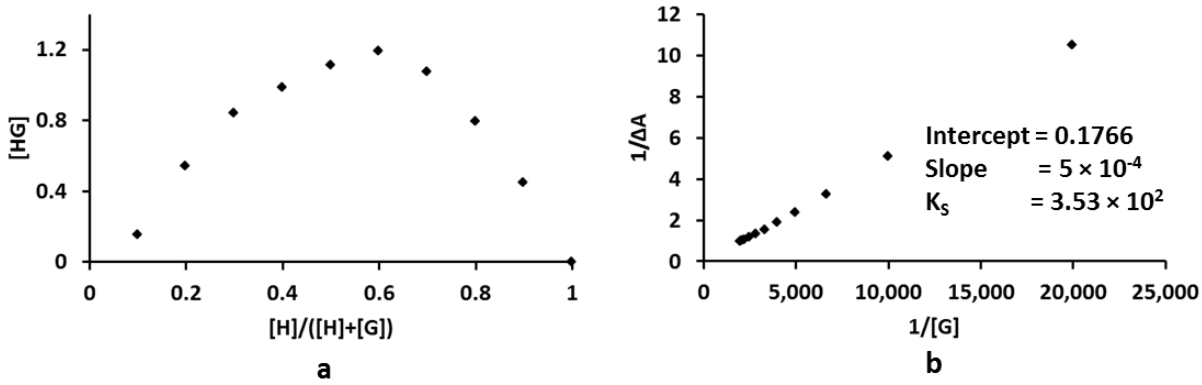

Fig. S26. Showing Job's plot and stoichiometry for addition of TBACN to (5).

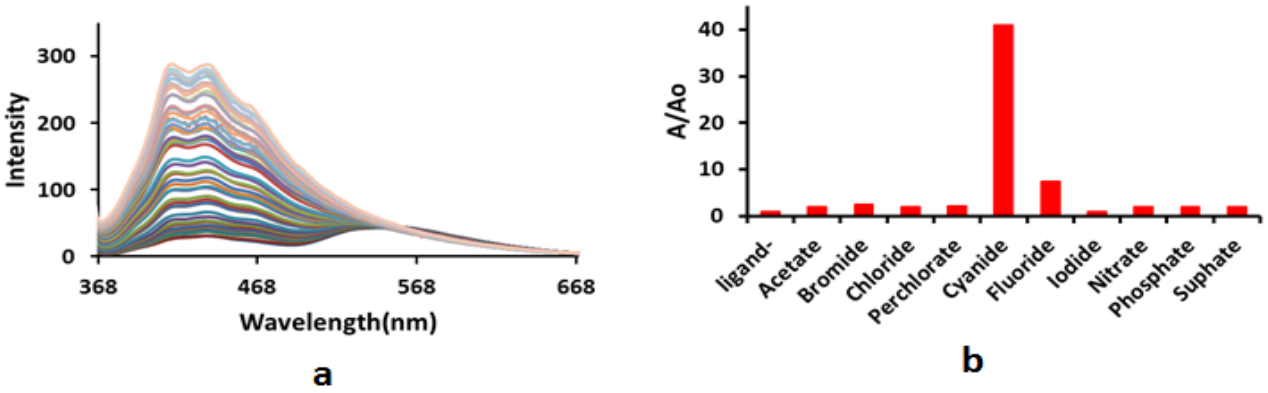

Fig. S27. Showing (a) changes in Fluorescence intensity of 443 nm band of (5) on addition of TBACN, Conc. (5) 5μM, anions (1-10 equivalents) (b) the relative changes in intensity with various anions.

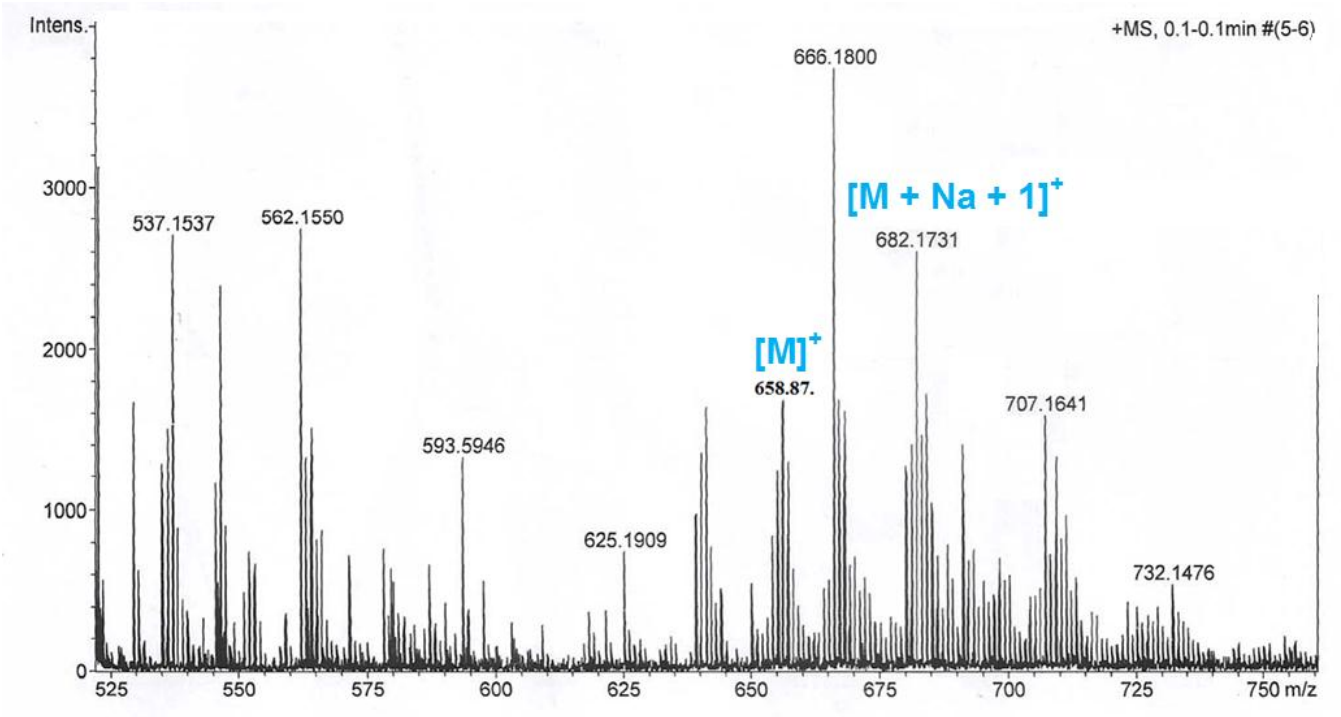

Fig. S28. ESIMS of CN adduct (7) obtained on addition of TBACN in (5) in DMSO.

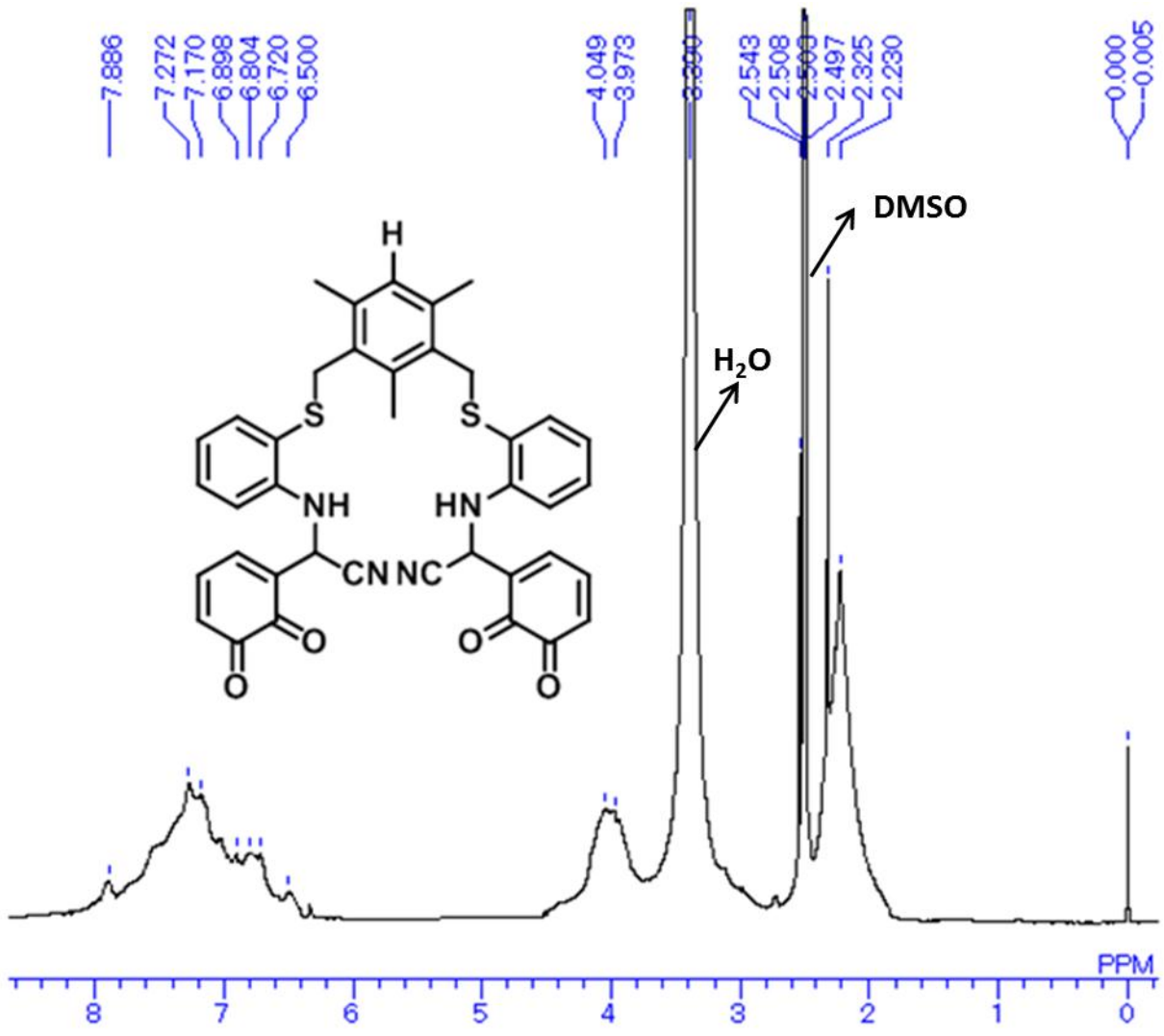

Fig. S29. ^{1}H NMR Spectrum of Compound 6. As the product 6 is a mixture of diastereomers therefore signals in the spectra can't be resolved completely. But all the required peaks are there in the spectrum.

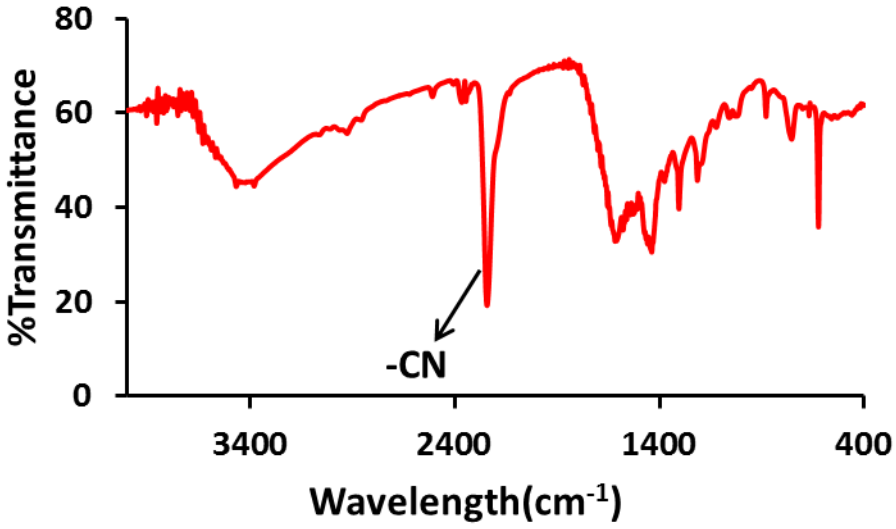

Fig. S30. IR Spectrum of Compound 6.

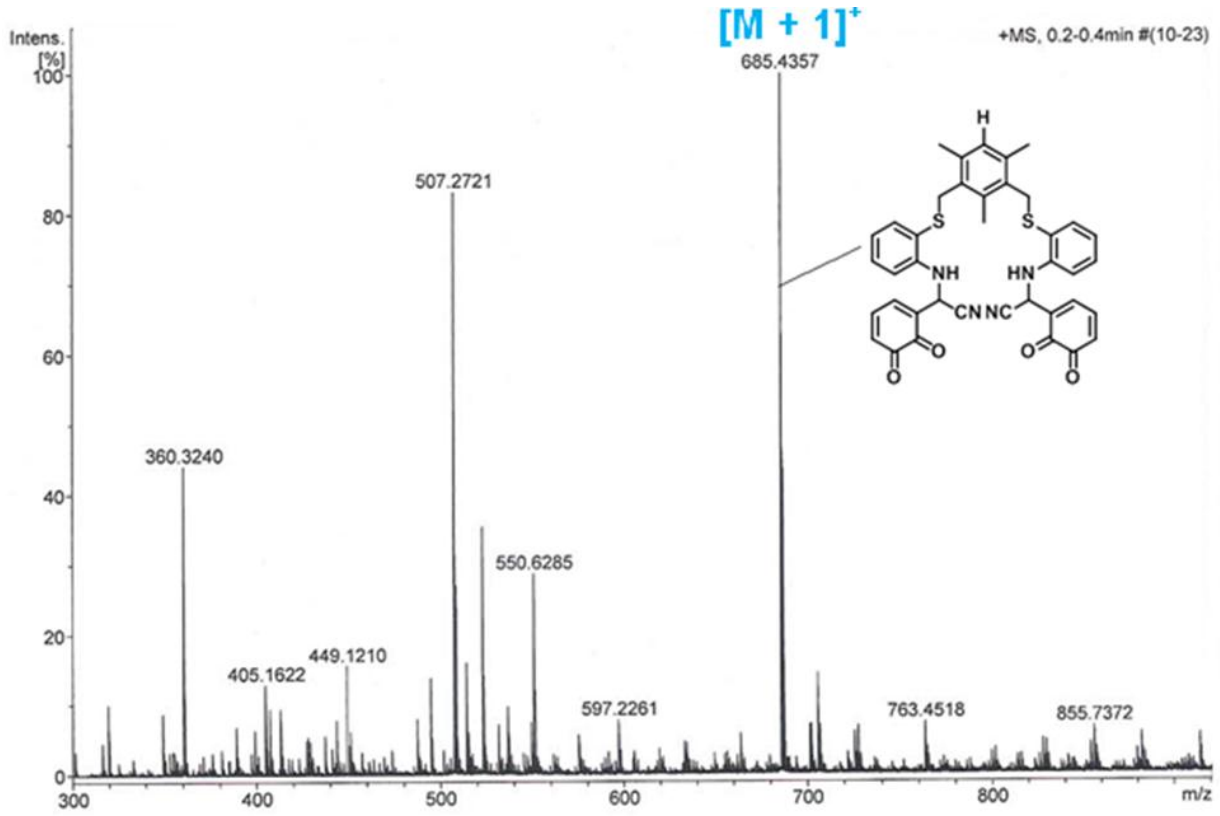

Fig. S31. Mass Spectrum of Compound 6.

Table 1. Crystal data and structure refinement for (**5**).

Identification code	shelxl	
Empirical formula	C112 H102 Cl4 N6 O6 S6	
Formula weight	1962.16	
Temperature	296(2) K	
Wavelength	0.71069 Å	
Crystal system	Rhombohedral	
Space group	R -3	
Unit cell dimensions	a = 23.896(7) Å	a= 90.0°.
	b = 23.896(7) Å	b= 90.0°.
	c = 30.268(9) Å	g = 120.0°.
Volume	14968(8) $Å^3$	
Z	6	
Density (calculated)	1.306 Mg/m^3	
Absorption coefficient	0.303 mm^{-1}	
F(000)	6168	
Crystal size	0.19 x 0.17 x 0.10 mm^3	
Theta range for data collection	1.19 to 25.00°.	
Index ranges	-28<=h<=28, -28<=k<=27, -30<=l<=36	
Reflections collected	19836	
Independent reflections	5877 [R(int) = 0.0261]	
Completeness to theta = 25.00°	99.9 %	
Absorption correction	Semi-empirical from equivalents	
Max. and min. transmission	0.745 and 0.628	
Refinement method	Full-matrix least-squares on F^2	
Data / restraints / parameters	5877 / 5 / 417	
Goodness-of-fit on F^2	0.996	
Final R indices [I>2sigma(I)]	R1 = 0.0683, wR2 = 0.2042	
R indices (all data)	R1 = 0.1260, wR2 = 0.2613	
Largest diff. peak and hole	0.265 and -0.564 $e.Å^{-3}$	
CCDC Number	898519	